

Temperature evolution of physical parameters in the Inert Doublet Model

Dorota Sokołowska

University of Warsaw, Faculty of Physics, Warsaw, Poland

November 12, 2021

Abstract

Inert Doublet Model is a minimal extension of the Standard Model with the second scalar doublet that may provide a Dark Matter candidate. In this paper we consider different variants of the evolution of the Universe after inflation, that lead towards the Inert phase today. We extend our previous analysis, in particular by discussing the co-existence of minima and providing numerical examples of the evolutions of the mass parameters for the different types of the history of the Universe. We take into account the existing constraints, including the relic density data.

1 Introduction

The Inert Doublet Model (IDM) [1] is a Z_2 symmetric 2HDM, which for a special set of parameters may provide the Dark Matter (DM) candidate. The model contains two scalar $SU(2)$ doublets. One is a "standard" scalar (Higgs) doublet Φ_S , responsible for electroweak symmetry breaking and masses of fermions and gauge bosons as in the Standard Model (SM), with a Higgs particle h_S . The second one is a "dark" scalar doublet Φ_D , which does not receive vacuum expectation value (v.e.v.) and does not couple to fermions¹. In the model the following discrete symmetry of the Z_2 type, which we call *the D-symmetry*, is present²:

$$D : \quad \Phi_S \xrightarrow{D} \Phi_S, \quad \Phi_D \xrightarrow{D} -\Phi_D, \quad SM \xrightarrow{D} SM. \quad (1)$$

All the components of the dark doublet Φ_D are realized as the massive D -scalars: two charged D^\pm and two neutral ones D_H and D_A . By construction, they possess a conserved multiplicative quantum number, *the D-parity*, and therefore the lightest particle among them can be considered as a candidate for the DM particle.

In this paper we discuss the evolution of the Universe during its cooling down after inflation, following the approach presented in [2, 3, 4, 5]. As before, we assume that the current state of the Universe is described by IDM. In this analysis we include all existing constraints on the model, together with the corresponding energy relic density, calculated by us [6] using micrOMEGAs [7].

In sec. 2 we list the basic properties of IDM and discuss the relevant astrophysical and collider constraints. Sec. 3 contains the summary of the basic assumptions of our approach and extended analysis of the possible today's states and types of evolution, as compared to [5]. In particular we trace the co-existence of minima. In sec. 4 we provide numerical examples of temperature evolution of physical parameters, like masses.

¹Our notations are similar to those in the general 2HDM with the change $\Phi_1 \rightarrow \Phi_S$, $\Phi_2 \rightarrow \Phi_D$.

² SM denotes SM fermions ψ_f and gauge bosons.

2 IDM

2.1 Lagrangian

We consider an electroweak symmetry breaking (EWSB) via the Brout-Englert-Higgs-Kibble (BEHK) mechanism described by the Lagrangian

$$\mathcal{L} = \mathcal{L}_{gf}^{SM} + \mathcal{L}_H + \mathcal{L}_Y(\psi_f, \Phi_S), \quad \mathcal{L}_H = T - V. \quad (2)$$

Here, \mathcal{L}_{gf}^{SM} describes the $SU(2) \times U(1)$ Standard Model interaction of gauge bosons and fermions, which is independent on the realization of the BEHK mechanism. In the considered case the scalar Lagrangian \mathcal{L}_H contains the standard kinetic term T and the D -symmetric potential V , which can describe IDM, with two scalar doublets Φ_S and Φ_D :

$$V = -\frac{1}{2} \left[m_{11}^2 \Phi_S^\dagger \Phi_S + m_{22}^2 \Phi_D^\dagger \Phi_D \right] + \frac{1}{2} \left[\lambda_1 \left(\Phi_S^\dagger \Phi_S \right)^2 + \lambda_2 \left(\Phi_D^\dagger \Phi_D \right)^2 \right] \\ + \lambda_3 \left(\Phi_S^\dagger \Phi_S \right) \left(\Phi_D^\dagger \Phi_D \right) + \lambda_4 \left(\Phi_S^\dagger \Phi_D \right) \left(\Phi_D^\dagger \Phi_S \right) + \frac{1}{2} \lambda_5 \left[\left(\Phi_S^\dagger \Phi_D \right)^2 + \left(\Phi_D^\dagger \Phi_S \right)^2 \right]. \quad (3)$$

All parameters in V are taken to be real, with $\lambda_5 < 0$ [5]. For the further discussion, it is useful to introduce the (μ_1, μ_2) phase space with:

$$\mu_1 = m_{11}^2 / \sqrt{\lambda_1}, \quad \mu_2 = m_{22}^2 / \sqrt{\lambda_2}. \quad (4)$$

Positivity conditions imposed on the potential guarantee the existence of the stable vacuum. They assure that the potential is bounded from below, meaning that the extremum with the lowest energy will be the global minimum of the potential (vacuum). The positivity constraints relevant for this analysis are:

$$\lambda_1 > 0, \quad \lambda_2 > 0, \quad R + 1 > 0, \quad (5)$$

$$R = \lambda_{345} / \sqrt{\lambda_1 \lambda_2}, \quad \lambda_{345} = \lambda_3 + \lambda_4 + \lambda_5. \quad (6)$$

\mathcal{L}_Y describes the Yukawa interaction of SM fermions ψ_f with only one scalar doublet Φ_S , having the same form as in the SM with the change $\Phi \rightarrow \Phi_S$ (Model I for a general 2HDM). For quarks it reads:

$$\mathcal{L}_Y = \bar{Q}_L \Gamma \Phi_S d_R + \bar{Q}_L \Delta \tilde{\Phi}_S u_R + (h.c.), \quad (7)$$

where Q_L is doublet of left-handed quarks, d_R, u_R are the right-handed quarks, Γ and Δ are 3×3 matrices of Yukawa couplings in generations space, $\tilde{\Phi} = i\sigma_2 \Phi^*$. Similar Yukawa term is introduced for leptons, namely $\bar{L}_L \Gamma \Phi_S l_R + (h.c)$. \mathcal{L}_Y respects D -symmetry in any order of the perturbation theory.

2.2 Inert vacuum state

Inert extremum, denoted by I_1 , is realized if the extremum conditions for the potential V respect

$$v^2 = \mu_1 / \sqrt{\lambda_1}. \quad (8)$$

I_1 realizes vacuum if following conditions are satisfied [5]:

$$\mu_1 > 0 \text{ for any } R, \quad \mu_1 > \mu_2 \text{ for } R > 1, \quad R\mu_1 > \mu_2 \text{ for } |R| < 1. \quad (9)$$

There are four dark scalar particles D_H, D_A, D^\pm and the Higgs particle h_S which interacts with the fermions and gauge bosons just as the Higgs boson in the SM.

Inert state is invariant under the D -transformation just as the whole basic Lagrangian (2) does. Therefore, the D -parity is conserved and due to this fact the lightest D -odd particle is stable, being a good DM candidate.

Masses of the scalar particles are:

$$\begin{aligned} M_{h_s}^2 &= \lambda_1 v^2 = m_{11}^2, & M_{D^\pm}^2 &= \frac{\lambda_3 v^2 - m_{22}^2}{2}, \\ M_{D_A}^2 &= M_{D^\pm}^2 + \frac{\lambda_4 - \lambda_5}{2} v^2, & M_{D_H}^2 &= M_{D^\pm}^2 + \frac{\lambda_4 + \lambda_5}{2} v^2. \end{aligned} \quad (10)$$

Assuming, as usual, that DM particles are neutral, we consider such variant of IDM, in which

$$M_{D^\pm}, M_{D_A} > M_{D_H}. \quad (11)$$

After EWSB parameters of the potential V can be expressed by the four scalar masses and two self-couplings λ_{345} , λ_2 between the neutral scalar particles. *Triple and quartic* couplings between SM-like Higgs h_S and DM candidate D_H , i.e. $D_H D_H h_S$ and $D_H D_H h_S h_S$, are proportional to λ_{345} . The second coupling, λ_2 , is related only to a *quartic* self-coupling, $D_H D_H D_H D_H$. The remaining self-coupling, λ_3 , governs the charged scalars' interactions: $D^+ D^- h_S$ and $D^+ D^- h_S h_S$.

2.3 Constraints

Various theoretical and experimental constraints apply for the IDM (see e.g. [8]-[12]).

The value of λ_{345} strongly affects the DM interactions relevant for the DM energy relic density $\Omega_{DM} h^2$. In general, for larger $|\lambda_{345}|$ the relic density decreases due to the enhanced $D_H D_H$ annihilation via s-channel Higgs exchange. This parameter also plays an important role in the indirect detection of DM [9, 10] and larger $|\lambda_{345}|$ gives an enhanced flux of neutrinos and gamma rays.

The value of the remaining coupling, λ_2 , does not influence the DM relic density explicitly and so this parameter is usually fixed to arbitrary small value during the DM analysis of IDM [9, 10]. However, value of λ_2 limits the value of λ_{345} via the positivity constraints ($\lambda_2 > |\lambda_{345}|/\sqrt{\lambda_1}$) and therefore it plays an important role in the analysis, as discussed in [6].

Collider constraints on scalars' masses Electroweak precision tests constrain strongly physics beyond SM. For IDM both light and heavy Higgs particle is allowed [1]. Constraints on the mass splittings $\delta_A = M_{D_A} - M_{D_H}$, $\delta_\pm = M_{D^\pm} - M_{D_H}$ have been discussed in [9]. For a light Higgs boson, the allowed region corresponds to $\delta_\pm \sim \delta_A$ with mass splittings that could be large. For heavy SM Higgs large δ_\pm is needed, while δ_A could be small. In this work we limit ourselves to the light SM-like Higgs boson.

As D^\pm, D_A and D_H do not couple to fermions, the LEP limits based on Yukawa interaction for the standard 2HDM don't apply. However, the signatures are similar to neutralinos and charginos interactions in MSSM and the absence of a signal at LEP II was interpreted within the IDM in paper [11]. This analysis excludes the following region of masses: $M_{D_H} < 80$ GeV, $M_{D_A} < 100$ GeV and $\delta_A > 8$ GeV. For $\delta_A < 8$ GeV the LEP I limit $M_{D_H} + M_{D_A} > M_Z$ applies.

Constraints on self-couplings The positivity constraints are imposed directly on quartic parameters in the potential (5,6). If we want to assure the perturbativity of the theory, self-couplings λ cannot be large. The bound (called *perturbativity constraint*) is set typically to

$$|\lambda| < 4\pi. \quad (12)$$

Astrophysical estimations of the energy relic density $\Omega_{DM} h^2$ may be used to give the limitations for $|\lambda_{345}|$ depending on the chosen value of masses of D_H and other scalars [9, 10]. However, they do not directly constrain the remaining quartic coupling λ_2 .

DM relict density constraints The DM energy density in the Universe is estimated to [13]:

$$\Omega_{DM}h^2 = 0.112 \pm 0.009. \quad (13)$$

In this analysis we assume that D_H is a dominant component of the observed DM and density (13) is today's density of D_H .

Various studies [9, 10] and our independent analysis show that for IDM there are three allowed regions of M_D : (i) light DM particles with mass close to and below 10 GeV, (ii) medium mass regime of 40 – 80 GeV and (iii) heavy DM of mass larger than 500 GeV. For purpose of this paper we concentrate on the medium mass region with the chosen set of masses (sec.4). With this choice parameters λ_2 and λ_{345} are free (up to the limitations discussed above). We consider different variants of their choice corresponding to different types of the evolution of the Universe.

For our analysis use of standard available tools, ie. micrOMEGAs, is in fact limited, as this program neglects temperature dependence of physical parameters and a possibility of more than one phase transition. In paper [5] we concluded that if in the past there were sequences of phase transitions, then the Universe entered the inert phase with DM candidate at lower temperatures than in one-stage EWSB. This should be taken into account while solving the Boltzmann equations for DM relict density n_D . Furthermore, one should consider the latent heat of the first order transition or strong fluctuations in the sequences of the second order phase transitions [14]. For a single phase transition the use of present form of micrOMEGAs is more justified, however taking into account the evolution of masses and existence of different decay channels may provide corrections. In this sense, the relict density calculations in this paper should be considered as a preliminary estimate.

3 Thermal evolution of the Universe

We consider thermal evolution of the Lagrangian, following the approach presented in [4, 3, 5]. It allows to study the earlier history of the Universe after inflation. In the first nontrivial approximation the Yukawa couplings and the quartic coefficients λ 's remain unchanged, while the mass parameters m_{ii}^2 ($i = 1, 2$) vary with temperature T as follows³:

$$m_{ii}^2(T) = m_{ii}^2 - c_i T^2, \quad (14)$$

$$c_1 = \frac{3\lambda_1 + 2\lambda_3 + \lambda_4}{6} + \frac{3g^2 + g'^2}{8} + \frac{g_t^2 + g_b^2}{2}, \quad c_2 = \frac{3\lambda_2 + 2\lambda_3 + \lambda_4}{6} + \frac{3g^2 + g'^2}{8}.$$

Here g and g' are the EW gauge couplings, while g_t and g_b are the SM Yukawa couplings for t and b quarks, respectively⁴.

In virtue of positivity conditions the sum of evolution coefficients is positive: $c_2 + c_1 > 0$. For $R > 0$ both $c_i > 0$, while for $R < 0$ arbitrary signs of $c_{1,2}$ are possible. In this work we limit ourselves to positive c_1, c_2 as we consider only the restoration of EW symmetry for high T (this corresponds to the negative values of $m_{11}^2(T)$, $m_{22}^2(T)$ for high enough T) [15]. See [5] for more details.

3.1 Possible minima during evolution

As the Universe is cooling down the potential V (3), with temperature dependent quadratic coefficients (14), may have different ground states. The general possible extrema are in form:

$$\langle \Phi_S \rangle = \frac{1}{\sqrt{2}} \begin{pmatrix} 0 \\ v_S \end{pmatrix}, \quad \langle \Phi_D \rangle = \frac{1}{\sqrt{2}} \begin{pmatrix} u \\ v_D \end{pmatrix}, \quad (15)$$

with $v_S > 0$ and $v^2 = v_S^2 + |v_D|^2 + u^2$.

³Formulae for c_1, c_2 were obtained recently by G. Gil (Master Thesis, 2011); they correct the corresponding formulae given in [5].

⁴Normalization of couplings: $g_i = \sqrt{2}m_i/v$, ($g_t \approx 0.99, g_b \approx 0.02$); $g = 2M_W/v = 0.652, g' = 0.351$.

Extrema and vacua		
name of extremum	properties of vacuum	vev's
<i>EW symmetric: EWs</i>	Massless fermions and bosons and massive scalar doublets.	$v_D = 0, \quad v_S = 0$
<i>inert: I₁</i>	Massive fermions and gauge bosons; scalar sector: SM-like Higgs h_S and dark scalars D_H, D_A, D^\pm with DM candidate D_H .	$v_D = 0,$ $v_S^2 = v^2 = \frac{\mu_1}{\sqrt{\lambda_1}}$
<i>inertlike: I₂</i>	Massless fermions and massive gauge bosons; scalar sector: Higgs particle h_D (no interaction with fermions), four scalars S_H, S_A, S^\pm , no DM candidate .	$v_S = 0,$ $v_D^2 = v^2 = \frac{\mu_2}{\sqrt{\lambda_2}}$
<i>mixed: M</i>	Massive fermions and bosons, 5 Higgs particles: CP-even h and H , CP-odd A and charged H^\pm , no DM candidate .	$v^2 = v_S^2 + v_D^2,$ $v_S^2 = \frac{\mu_1 - R\mu_2}{\sqrt{\lambda_1}(1 - R^2)} > 0,$ $v_D^2 = \frac{\mu_2 - R\mu_1}{\sqrt{\lambda_2}(1 - R^2)} > 0$

Table 1: General properties of the extrema and vacua, following [5].

Possible neutral solutions ($u = 0$) are: EW symmetric *EWs*, inert I_1 , inertlike I_2 and mixed M . Their general properties are summarized in table 1 [5], see also the appendix A.

There are three distinguish allowed regions of parameters λ 's, the best parametrized by the parameter R (6), namely a) $R > 1$, b) $1 > R > 0$, c) $0 > R > -1$.

The EW symmetric state (*EWs*) exists for every value of R if and only if both $\mu_1 < 0$ and $\mu_2 < 0$, being the only existing extremum (and thus the vacuum). For $R > 1$ (fig.1a) the energy of the mixed extremum M (if it exists) is always higher than for the other extrema, so it cannot be the vacuum [5]. Possible *EWv* vacua in this case are I_1 and I_2 . Fig.1b shows the allowed regions for $0 < R < 1$. Again we have the regions of *EWs*, I_1 and I_2 vacua, but now also mixed extremum M can be realized as a vacuum. Case of $R < 0$ is similar to the previous one but with the wider region of M vacuum (fig.1c). Summary of existing extrema, local minima and vacua for various R regions can be found in table 2.

3.2 Possible sequences of phase transitions

We use $(\mu_1(T), \mu_2(T))$ phase diagrams and the redefined evolution coefficients \tilde{c}_1, \tilde{c}_2 to determine the sequences of transitions between different vacua as T decreases:

$$\mu_1(T) = m_{11}^2(T)/\sqrt{\lambda_1}, \quad \mu_2(T) = m_{22}^2(T)/\sqrt{\lambda_2}, \quad (16)$$

$$\tilde{c}_1 = c_1/\sqrt{\lambda_1}, \quad \tilde{c}_2 = c_2/\sqrt{\lambda_2}, \quad \tilde{c} = \tilde{c}_2/\tilde{c}_1. \quad (17)$$

Figs.(1a,b,c) show all possible types of evolution from the EW symmetric phase towards the inert phase today. The possible evolutions are represented by the rays directed towards the growth of time, ie. the decrease of the temperature. Today's values are defined by $\mu_1 = \mu_1(0), \mu_2 = \mu_2(0)$ and marked by dots in figures.

The relevant temperatures with the corresponding conditions for the phase transitions are [5]:

a) Extrema and vacua for $R > 1$	
$\mu_2 > 0$ and $\mu_2 > \mu_1 R$	I_2 is the vacuum. For $\mu_1 > 0$ I_1 is an extremum, but not a minimum.
$0 < \mu_1 < \mu_2 < \mu_1 R$	I_2 is the vacuum (i.e. global minimum) and I_1 – a local minimum.
$0 < \mu_1 R^{-1} < \mu_2 < \mu_1$	I_1 is the vacuum (i.e. global minimum) and I_2 – a local minimum.
$\mu_1 > 0$ and $\mu_2 < \mu_1 R^{-1}$	I_1 is the vacuum. For $\mu_2 > 0$ I_2 is an extremum, but not a minimum.
b) Extrema and vacua for $1 > R > 0$	
$\mu_2 > 0$ and $\mu_2 > \mu_1 R^{-1}$	I_2 is the vacuum. For $\mu_1 > 0$ I_1 is an extremum, but not a minimum.
$\mu_1 > 0$ and $\mu_2 < \mu_1 R$	I_1 is the vacuum. For $\mu_2 > 0$ I_2 is an extremum, but not a minimum.
$0 < \mu_1 R < \mu_2 < \mu_1 R^{-1}$	M is the vacuum, I_1 and I_2 are the extrema.
c) Extrema and vacua for $0 > R > -1$	
$\mu_2 > 0$ and $\mu_2 < \mu_1 R^{-1}$	I_2 is the vacuum, no other extrema.
$\mu_1 > 0$ and $\mu_2 < \mu_1 R$	I_1 is the vacuum, no other extrema.
$\mu_2 > \text{Max}(\mu_1 R^{-1}, \mu_1 R)$	M is the vacuum. Extrema: I_2 for $\mu_2 > 0$, I_1 for $\mu_1 > 0$.

Table 2: EWv extrema and vacua for various R regions.

$$T_{EWs,1} = \sqrt{\mu_1/\tilde{c}_1} \quad (\mu_1(T_{EWs,1}) = 0), \quad (18)$$

$$T_{EWs,2} = \sqrt{\mu_2/\tilde{c}_2} \quad (\mu_2(T_{EWs,2}) = 0), \quad (19)$$

$$T_{2,1} = \sqrt{\frac{\mu_1 - \mu_2}{\tilde{c}_1 - \tilde{c}_2}} \quad (\mu_1(T_{2,1}) = \mu_2(T_{2,1})), \quad (20)$$

$$T_{2,M} = \sqrt{\frac{\mu_1 - R\mu_2}{\tilde{c}_1 - R\tilde{c}_2}}, \quad T_{M,1} = \sqrt{\frac{R\mu_1 - \mu_2}{R\tilde{c}_1 - \tilde{c}_2}}, \quad (21)$$

$$(\mu_2(T_{2,M}) = \mu_1(T_{2,M})/R, \quad \mu_1(T_{M,1}) = \mu_2(T_{M,1})/R).$$

3.2.1 $R > 1$

For $R > 1$ the possible types of evolution that lead towards the inert phase today can be divided into two groups (fig.1a, table 3). The first one corresponds to a single phase transition of the 2nd-order at the temperature (18), shown by rays Ia, IIa and III. The second type of evolution is in form of a sequence of two phase transitions represented by the rays IV and V. For these rays, the first phase transition $EWs \rightarrow I_2$ (EWsB) realized at temperature (19) is a 2nd-order phase transition, while the second one $I_2 \rightarrow I_1$, realized at temperature (20), is a 1st-order transition.

We notice that the considered $R > 1$ case contains an unique opportunities of co-existing minima (vacuum I_1 and local metastable minimum I_2) for rays III, IV and V. Also, only in this case there is a possibility of the 1st-order phase transition (rays IV and V). That cannot be realized for the other values of R . For ray IV the co-existence is temporary and the local minimum I_2 disappear for low temperatures, while for rays III and V it still exists for $T = 0$.

For $R = 1$ the phase space of co-existing minima I_1 and I_2 is reduced to line $\mu_1(T) = \mu_2(T)$. Here rays III and V are not possible, unless additional condition of $\mu_1 = \mu_2$ is fulfilled. That however leads to the existence of two degenerate minima for $T = 0$.

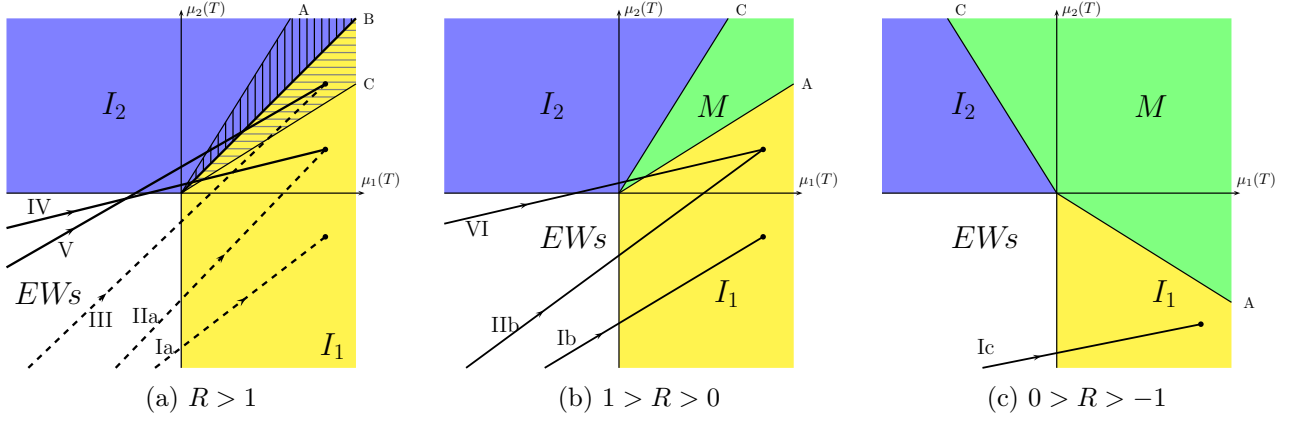


Figure 1: Possible vacua and evolution to a current states (dots) represented by rays on (μ_1, μ_2) plane for a) $R > 1$, b) $1 > R > 0$, c) $0 > R > -1$. The boundary lines are $A : \mu_2 = \mu_1 R$, $B : \mu_2 = \mu_1$, $C : \mu_2 = \mu_1/R$. Blue (dark shade) region represents I_2 vacuum, yellow (light shade) region – I_1 vacuum and green (medium shade) region – M vacuum. In the hatched regions between lines A, B and B, C I_1 and I_2 minima co-exist.

If $\tilde{c} \neq 1$ then after EWSB only one EWv minimum is created (either I_1 or I_2). However, there is a possibility that $\tilde{c} = 1$ and $\mu_1 = \mu_2$. In this case after EWSB two degenerate minima appear and they have the same energy for the whole time after symmetry breaking. Note, that because of the form of Yukawa interaction the fermionic contribution appears only in c_1 and so $\tilde{c} = 1$ is possible only if $\lambda_1 \neq \lambda_2$.

Ray	Sequence	Conditions	Co-existing min. and extr. for $T = 0$
Ia	$EWs \rightarrow I_1$	$\mu_2 < 0$	-
IIa	$EWs \rightarrow I_1$	$0 < \mu_2 < \text{Min}(\mu_1 \tilde{c}, \mu_1 R^{-1})$	I_2 extremum
III	$EWs \rightarrow I_1$	$\mu_1 R^{-1} < \mu_2 < \text{Min}(\mu_1 \tilde{c}, \mu_1)$	I_2 local minimum
IV	$EWs \rightarrow I_2 \rightarrow I_1$	$\mu_1 \tilde{c} < \mu_2 < \mu_1 R^{-1}$	I_2 extremum
V	$EWs \rightarrow I_2 \rightarrow I_1$	$\text{Max}(\mu_1 \tilde{c}, \mu_1 R^{-1}) < \mu_2 < \mu_1$	I_2 local minimum

Table 3: Possible rays for $R > 1$.

3.2.2 $0 < R < 1$

In the $0 < R < 1$ case for every point in phase diagram $(\mu_1(T), \mu_2(T))$ there is only one existing minimum (and so it is a vacuum), as shown in fig.1b, and all transitions are of the 2nd-order. We can reach the today's inert phase by a single phase transition or through the sequence of three 2nd-order phase transitions (table 4). First type of sequence $EWs \rightarrow I_1$ is realized by rays Ib and IIb, which are the analogs of rays Ia and IIIb. For ray VI, which corresponds to the sequence $EWs \rightarrow I_2 \rightarrow M \rightarrow I_1$, EWSB happens at temperature (19). Then there are two more transitions in this sequence: from I_2 into M and from M into the inert vacuum I_1 , with the last transition at temperature (21).

Ray no.	Sequence	Conditions	Co-existing min. and extr. for $T = 0$
Ib	$EW_s \rightarrow I_1$	$\mu_2 < 0$	-
IIb	$EW_s \rightarrow I_1$	$0 < \mu_2 < \text{Min}(\mu_1 \tilde{c}, \mu_1 R)$	I_2 extremum
VI	$EW_s \rightarrow I_2 \rightarrow M \rightarrow I_1$	$\mu_1 \tilde{c} < \mu_2 < \mu_1 R$	I_2 extremum

Table 4: Possible rays for $1 > R > 0$.

3.2.3 $-1 < R < 0$

We consider the restoration of EW symmetry in the past (both c_1, c_2 positive) and there is only one possible ray Ic, which is similar to the rays Ia and Ib (table 5, fig.1c) [5].

Ray no.	Sequence	Conditions	Co-existing min. and extr. for $T = 0$
Ic	$EW_s \rightarrow I_1$	$\mu_2 < \mu_1 R < 0$	-

Table 5: Possible rays for $0 > R > -1$.

4 Temperature evolution of physical parameters

In the previous sections to describe the history of the Universe we used the parameters of the Lagrangian, namely μ_1, μ_2 and R, \tilde{c} . Relations between them gave us information about the possible sequences of the phase transitions. In this section we illustrate the underlying temperature evolutions of the physical parameters (i.e. masses of the particles) for various rays, each representing the different history of the Universe. Here, it is useful to fix six free parameters of the model in form of four physical masses

$$M_{h_S}, \quad M_{D_A}, \quad M_{D_H}, \quad M_{D^\pm} \quad (22)$$

and two self-couplings: λ_{345} and λ_2 . The considered values of masses and λ 's are chosen in agreement with existing constraints both from the colliders and the DM abundance measurements, as discussed in sec. 2.3. The values of $\Omega_{DM} h^2$ were calculated with the existing micrOMEGAs code. We expect the $\Omega_{DM} h^2$ to lie in the 3σ WMAP allowed range:

$$0.085 < \Omega_{DM} h^2 < 0.139. \quad (23)$$

As we treat those results as an estimate only the fact that for some rays the calculated value is slightly outside the this range does not exclude automatically those rays.

The following scalar mass set was used for the today's inert phase:

$$M_{h_S} = 120 \text{ GeV}, \quad M_{D_H} = 45 \text{ GeV}, \quad M_{D_A} = 115 \text{ GeV}, \quad M_{D^\pm} = 125 \text{ GeV}, \quad (24)$$

with self-couplings λ_{345} and λ_2 different for each ray [18]⁵.

Below we show mass evolutions arising from (14) represented by different rays for all three R regions: rays Ia, III, IV and V for $R > 1$, ray VI for $1 > R > 0$ and ray Ic for $R < 0$ (figs.2-7). We plot the temperature dependent masses of the scalars for every vacua that is realized for a chosen

⁵The detailed discussion of the importance and constraints of those couplings is in progress [6].

ray. We also present the temperature dependence of the ‘‘mass parameters’’ for scalar states of local minima. In addition we present dependence on the temperature of two other physical parameters, namely the top quark mass $m_t(T)$ and $v(T)$ (proportional to the W boson mass $M_W(T)$).

The initial state of the Universe is the EW symmetric phase with two massive scalar doublets Φ_S, Φ_D and massless both fermions as well as gauge bosons. In this vacuum there are eight massive scalar states that come from the two scalar doublets, denoted on plots by Φ_S, Φ_D , with masses equal to $|m_{11}(T)|/\sqrt{2}$, $|m_{22}(T)|/\sqrt{2}$, respectively. After EWSB the Universe enters one of the symmetry violating vacuum with the proper particle content, with masses described by the formulas presented in the appendix A.

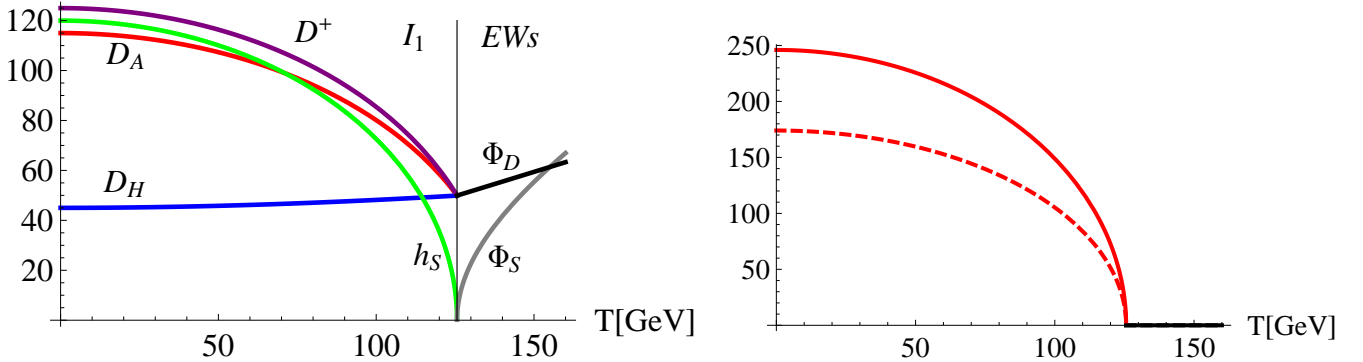
4.1 The $R > 1$ case

4.1.1 Ray Ia

Figs.(2a,b) show mass evolution for the ray Ia, corresponding to the single phase transition $EWs \rightarrow I_1$, for the following set of parameters:

$$\lambda_2 = 0.012, \quad \lambda_{345} = 0.065 \quad \Rightarrow \quad c_1 = 0.913, \quad c_2 = 0.309. \quad (25)$$

The EWSB happens at $T = 125.6$ GeV and Universe enters the phase with massive fermions and gauge bosons (fig.2b). The Universe stays in the I_1 phase with the mass of DM candidate nearly constant $M_{D_H}(T) \approx 45$ GeV, fig. 2a.



(a) masses of scalar states in I_1 : M_{D_H} (blue), M_{D_A} (red), M_{D^+} (purple), M_{h_S} (green) and EWs : Φ_D (black), Φ_S (grey) (b) $v(T)$ (solid) and $m_t(T)$ (dashed) for EWs (black) and I_1 (red)

Figure 2: Evolution of masses (ray Ia): $EWs \rightarrow I_1$.

4.1.2 Ray III

Ray III (figs.3a,b) can be realized for:

$$\lambda_2 = 0.02, \quad \lambda_{345} = 0.117 \quad \Rightarrow \quad c_1 = 0.93, \quad c_2 = 0.33. \quad (26)$$

Again here there is a single phase transition and after EWSB the Universe enters the I_1 phase at $T = 124.5$ GeV. This case is different from the previous one as at $T = 57$ GeV another minimum – local minimum I_2 – appears (shaded region in fig.3a). Dashed lines show the change of ‘‘mass parameters’’ for corresponding scalar states of this local minimum (see appendix A).

4.1.3 Ray IV

Figs.(4a,b) show the mass evolution for the ray IV, for the following set of parameters:

$$\lambda_2 = 0.068, \quad \lambda_{345} = 0.16 \quad \Rightarrow \quad c_1 = 0.944, \quad c_2 = 0.368. \quad (27)$$

The EWSB happens at $T = 123.6$ GeV when Universe enters the inertlike phase I_2 with massless fermions and massive gauge bosons (fig.4b). As the time grows another extremum appears, which later becomes a local minimum I_1 . The first-order phase transition $I_2 \rightarrow I_1$ happens at $T = 123.1$ GeV. Note, that two minima coexist during a period of time $\Delta T \approx 1.5$ GeV (shown by the shaded region in fig.4a). The "mass parameters" of the scalar states in the *local* minima I_1 and I_2 are shown. The discontinuity in masses of physical particles: scalars, fermions and gauge boson (proportional to v) is visible. Universe enters the inert phase I_1 with massive fermions, gauge bosons and scalars, among them with DM candidate D_H and their mass evolution continues up to the $T = 0$ mass values.

4.1.4 Ray V

Figs.(5a,b) show ray V, which can be realized for the following parameters:

$$\lambda_2 = 0.05, \quad \lambda_{345} = 0.17 \quad \Rightarrow \quad c_1 = 0.948, \quad c_2 = 0.363. \quad (28)$$

First, there is EWSB into the I_2 phase at $T = 131$ GeV. Then at $T = 113.5$ GeV the local minimum I_1 appears. The first order $I_2 \rightarrow I_1$ transition happens at $T = 71$ GeV, and I_2 becomes a local minimum, which does not disappear up to $T = 0$. These two minima coexist during a period represented by the shaded region in fig.5a. Dashed lines correspond to the "mass parameters" of the scalar states in the *local* minima I_1 and I_2 . Note, that for this ray the final phase transition happens at the lower temperatures than in the other cases, where ratio $M_{D_A, D^\pm}/T$ is of the order 1.

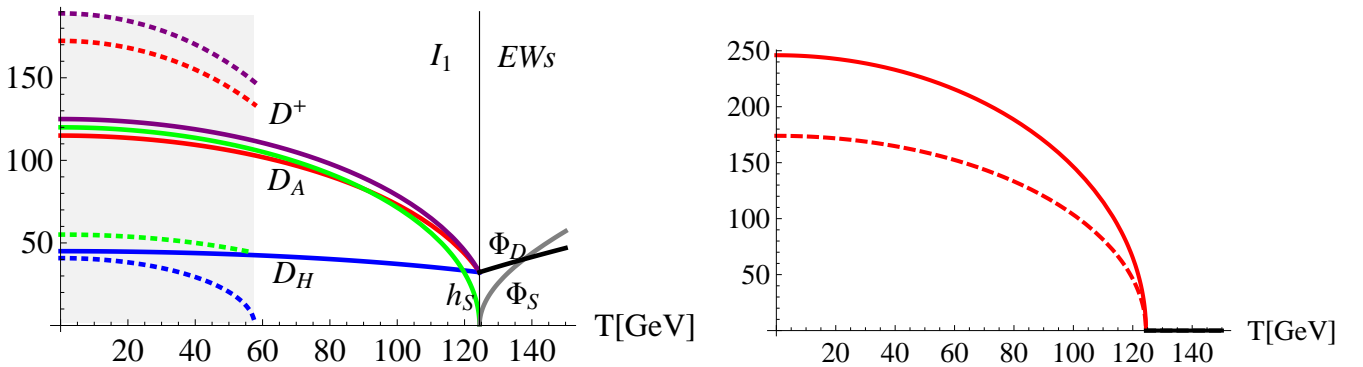
4.2 The $1 > R > 0$ case

4.2.1 Ray VI

Figs.(6a,b) show the evolution of the Universe along the ray VI. At every temperature there is only one minimum, all three transitions are of the 2nd-order. We study mass evolutions for:

$$\lambda_2 = 0.125, \quad \lambda_{345} = 0.17 \quad \Rightarrow \quad c_1 = 0.947, \quad c_2 = 0.40. \quad (29)$$

EWSB happens at $T = 124.8$ GeV. Universe enters the inertlike phase I_2 with massless fermions and massive gauge bosons (fig.6b). At $T = 121.1$ GeV the mass of S_H particle goes to 0 and the 2nd-order transition to the M phase takes place. This phase is very short lived, at the beginning and at the end the mass of h particle goes to zero, at $T = 121.1$ GeV and $T = 120.9$ GeV, respectively. At this last 2nd-order transition Universe enters the inert phase I_1 with the DM candidate D_H . The mass evolution continues to the today's values of masses. Note, that here rays V and VI have the same λ_{345} , while they differ by the value of λ_2 .



(a) masses of scalars in I_1 : M_{D_H} (blue), M_{D_A} (red), M_{D^+} (purple), M_{h_S} (green) and EWs : Φ_D (black), Φ_S (grey). Dashed lines – mass parameters of local I_2 . Shaded region – local minimum I_2 .

(b) $v(T)$ (solid) and $m_t(T)$ (dashed) for EWs (black) and I_1 (red)

Figure 3: Evolution of masses (ray III): $EWs \rightarrow I_1$.

4.3 The case $0 > R > -1$

4.3.1 Ray Ic

Ray Ic shown in figs.(7a,b) is realized for:

$$\lambda_2 = 0.1, \quad \lambda_{345} = -0.115 \quad \Rightarrow \quad c_1 = 0.852, \quad c_2 = 0.293. \quad (30)$$

In this case there is a single phase transition (EWSB) at $T = 130$ GeV. Universe enters the inert phase I_1 with massive fermions, gauge bosons and DM candidate D_H .

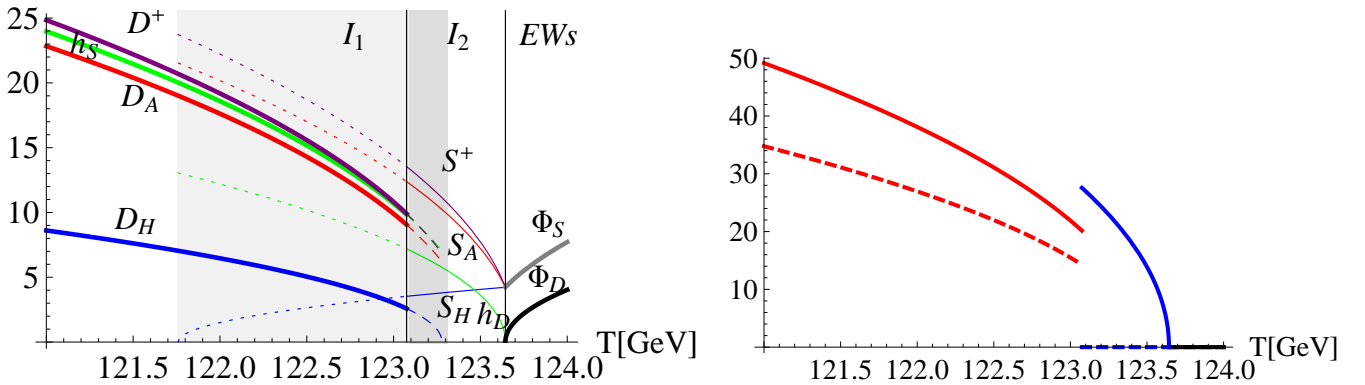
4.4 Relict densities for considered rays

We use the micrOMEGAs code [7] for a rough estimation of the relict density for the rays described in the previous sections 4.1-4.3. Results for $\Omega_{DM}h^2$ are presented in fig.8, where dots represent values obtained for the different rays. Ray Ia with $\Omega_{DM}h^2 = 0.31$ is excluded by the WMAP results. For rays Ic and III values of $\Omega_{DM}h^2$ are within the WMAP range. As $|\lambda_{345}|$ grows the observed $\Omega_{DM}h^2$ decreases and for rays IV, V and VI it is below the lower WMAP limit. $\Omega_{DM}h^2$ for rays VI and V are equal, as those rays differ only by the value of λ_2 , which does not enter explicitly the rates for processes relevant for the DM abundance.

As discussed before, those values are an estimate of the real relict density. Sizable corrections are expected especially for ray V, because in this case the temperature of the final phase transition (1st-order) is the lowest.

Fig.8 contains $\Omega_{DM}h^2$ as a function of λ_{345} . Calculation was done for $\lambda_2 = 0.15$. Although Ω_{DM} does not depend explicitly of the value of λ_2 , its value limits the range of λ_{345} we can scan over because of the positivity constraints and necessary conditions for the inert minimum to be a global minimum [6]. In the considered case we can have the physical solutions only in range $0.2 > \lambda_{345} > -0.2$.

For the large mass splitting that we chose, the coannihilation is not important and the main process is $D_H D_H \rightarrow b\bar{b}$. For low values of $|\lambda_{345}|$ the relict density is high, as the annihilation via h_S is low. It becomes more important and it lowers the resulting $\Omega_{DM}h^2$ as $|\lambda_{345}|$ grows. We find that two λ_{345} regions, $\lambda_{345} \in (-0.105, -0.13), (0.105, 0.13)$, are in agreement with the WMAP limit (23).



(a) masses of scalar states around phase transitions for I_1 (thick lines) and I_2 (thin lines). Green – (h_S, h_D) , purple – (D^\pm, S^\pm) , red – (D_A, S_A) , blue – (D_H, S_H) . Dashed and dotted lines – local minima parameters. Shaded region – co-existence of minima I_1 and I_2 .

(b) $v(T)$ (solid) and $m_t(T)$ (dashed) for EWs (black), I_2 (blue) and I_1 (red)

Figure 4: Evolution of masses (ray IV): $EWs \rightarrow I_2 \rightarrow I_1$.

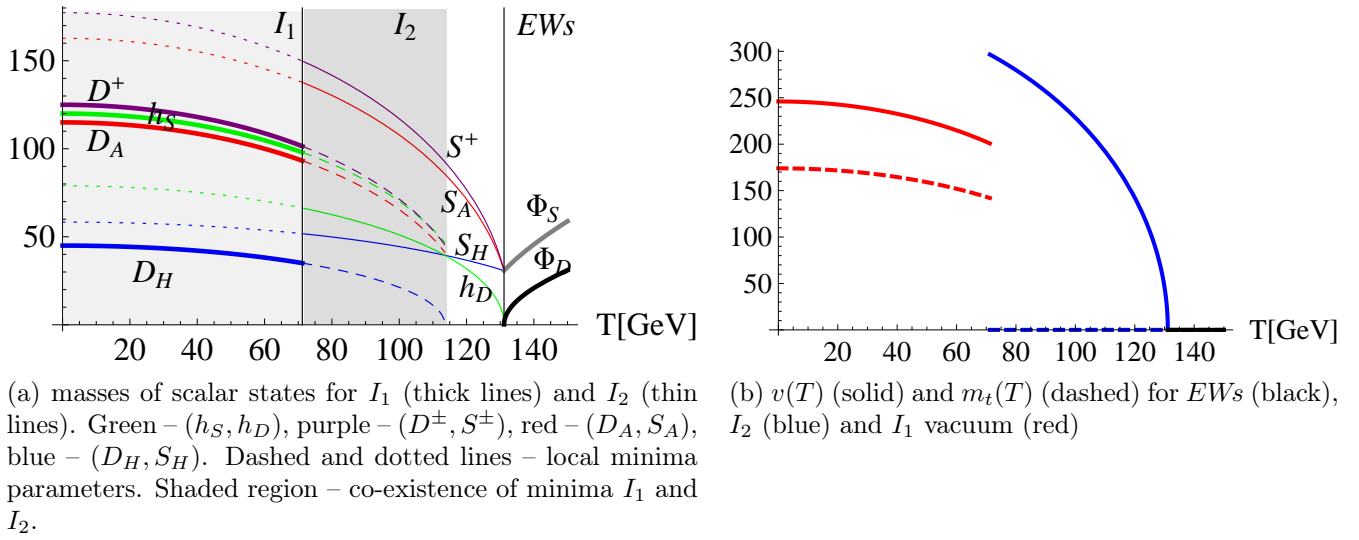


Figure 5: Evolution of masses (ray V): $EWs \rightarrow I_2 \rightarrow I_1$.

5 Discussion and conclusions

In this paper we studied further the evolution of the Universe after inflation towards the present inert phase. We considered different types of evolution, which may be parametrized by using the parameter R .

We extend the studies with respect to the previous paper [5] by discussing the possibility of co-existence of the local minima. This opportunity may be realized for two types of rays - ray IV and V. In the first case the co-existence is only temporary, as the phase transitions happen in a short period of time and the local minimum I_2 disappears shortly after the Universe enters the inert phase.

However, we find that also other situation is possible. For ray V the local minimum I_2 does not disappear and it exists for $T = 0$. Also for ray III, which corresponds to a single phase transition, the local minimum I_2 appears for the later stages of evolution and it exists for $T = 0$. Furthermore, this ray gives a good relict density.

We also stress the fact that the intermediate phases I_2, M for rays IV and VI are short-lived. In this sense those sequences may be considered as a similar to the one with the single phase transition, however the latent heat of the 1st-order phase transition may affect the evolution.

One should keep in mind the limitations of using micROMEGAs in the context of our analysis. First, we consider only the two body final states and so, for our mass range, the actual Ω_{DM} may be lower [19]. Furthermore, the temperature dependence of masses and the latent heat from the first

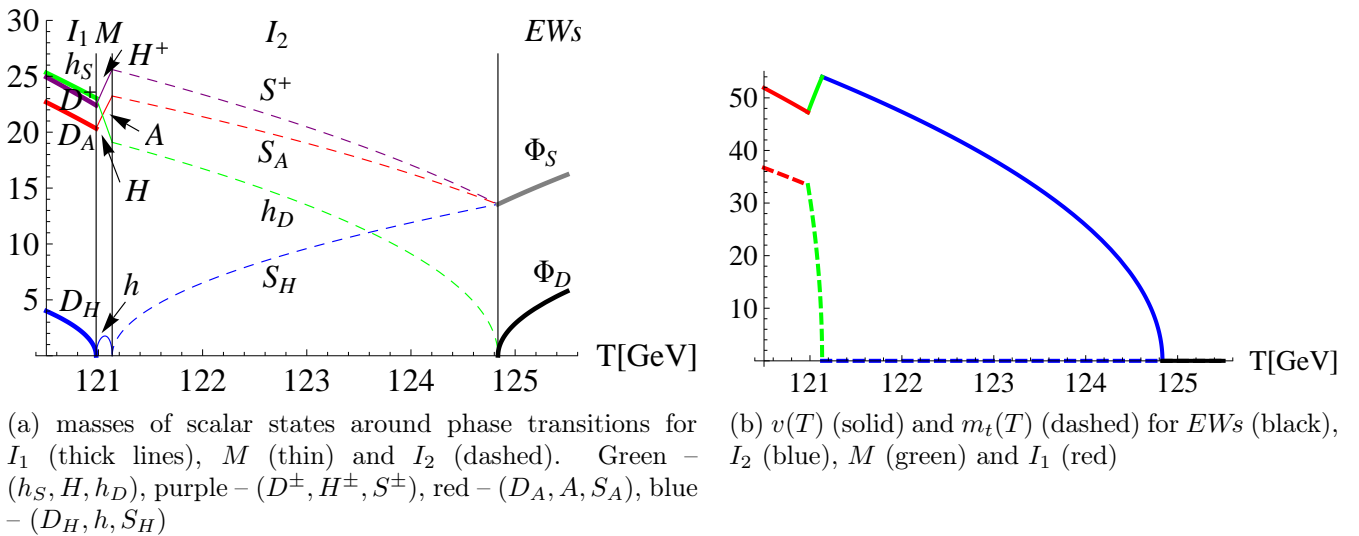


Figure 6: Evolution of masses (ray VI): $EWs \rightarrow I_2 \rightarrow M \rightarrow I_1$.

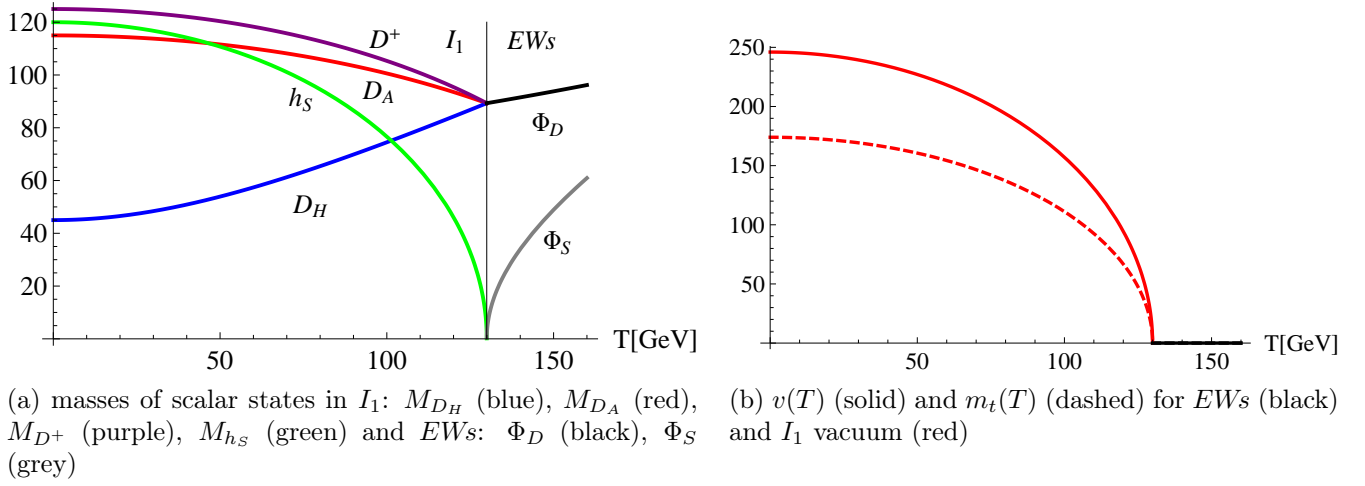


Figure 7: Evolution of masses (ray Ic): $EWs \rightarrow I_1$.

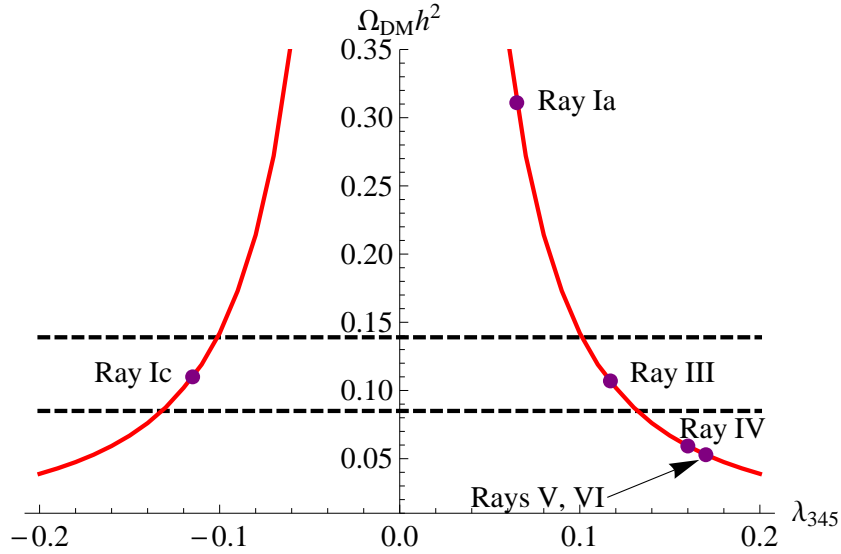


Figure 8: Relict density $\Omega_{DM}h^2(\lambda_{345})$ (red curve) with WMAP limits (dashed lines). Dots correspond to particular rays.

order phase transition will influence the value of $\Omega_{DM}h^2$. We expect that the relict density for rays IV-VI will be higher, as the final phase transition happens at the lower temperature than the EWSB for the other rays. The corrections from the 1st-order phase transition will result in the splitting between rays V and VI, which for now have the same relict density. We should also take into account the fact, that during the evolution the relation between the mass of the DM particle M_{D_H} and masses of the possible decay states (M_W, M_t, M_b) may vary. For certain rays decay channels other than $\bar{b}b$ may play important role and affect the energy relict density (for example, $D_H D_H \rightarrow WW$ for $M_{D_H}(T) > M_W(T)$). The detailed analysis of those effects is in preparation [14].

Acknowledgement I would like to thank I. Gizburg, K. Kanishev and M. Krawczyk for cooperation and discussions. We are thankful to P. Chankowski for discussions, to A. Pukhov and A. Belyaev for useful informations about micrOMEGAs package. Work was partly supported by Polish Ministry of Science and Higher Education Grant N N202 230337.

A Vacua properties

The neutral solution of extremum conditions give the following values of v_S, v_D parameters:

$$\mathbf{EWs} : \quad v_D = 0, \quad v_S = 0, \quad \mathcal{E}_{EWs} = 0; \quad (31)$$

$$\mathbf{I}_1 : \quad v_D = 0, \quad v_S^2 = v^2 = \frac{m_{11}^2}{\lambda_1}, \quad \mathcal{E}_{I_1} = -\frac{m_{11}^4}{8\lambda_1}; \quad (32)$$

$$\mathbf{I}_2 : \quad v_S = 0, \quad v_D^2 = v^2 = \frac{m_{22}^2}{\lambda_2}, \quad \mathcal{E}_{I_2} = -\frac{m_{22}^4}{8\lambda_2}; \quad (33)$$

$$\mathbf{M} : \quad v_S^2 = \frac{m_{11}^2 \lambda_2 - \lambda_{345} m_{22}^2}{\lambda_1 \lambda_2 - \lambda_{345}^2}, \quad v_D^2 = \frac{m_{22}^2 \lambda_1 - \lambda_{345} m_{11}^2}{\lambda_1 \lambda_2 - \lambda_{345}^2}; \quad (34)$$

$$\mathcal{E}_M = -\frac{m_{11}^4 \lambda_2 - 2\lambda_{345} m_{11}^2 m_{22}^2 + m_{22}^4 \lambda_1}{8(\lambda_1 \lambda_2 - \lambda_{345}^2)}.$$

Some of the equations (32)-(34) can give also negative values of v_S^2 or v_D^2 . In such case the extremum, described by corresponding equations, is absent.

A.1 EW symmetric vacuum EWs

The electroweak symmetric extremum EWs (31) is a minimum if $m_{11,22}^2 < 0$. Gauge bosons and fermions are massless, while the doublets have non-zero masses $\frac{|m_{11}^2|}{\sqrt{2}}$ and $\frac{|m_{22}^2|}{\sqrt{2}}$, respectively.

A.2 Inert-like vacuum I_2

The *inertlike vacuum* I_2 is "mirror-symmetric" to the inert vacuum I_1 , compare (32) and (33), with one Higgs particle h_D and four scalar particles: S_H, S_A, S^\pm . The interaction among scalars and between scalars and gauge bosons are mirror-symmetric as well, so the only difference between I_2 and I_1 arises from the Yukawa interaction.

The inertlike vacuum I_2 violates D -symmetry. The Higgs boson h couples to gauge bosons just as the Higgs boson of the SM, however it does not couple to fermions at the tree level. The scalars do interact with fermions. Therefore, here there are no candidates for dark matter particles. Note that all fermions, by definition interacting only with Φ_S with vanishing v.e.v. $\langle \Phi_S \rangle = 0$, are massless. (Small mass can appear only as a loop effect.)

The masses of the Higgs boson h_D and S -scalars are given by (cf. (10)) with $m_{11}^2 \leftrightarrow m_{22}^2$.

A.3 Mixed vacuum M

The mixed extremum⁶ M violates the Z_2 symmetry. In this vacuum we have massive fermions and no candidates for DM particle, like in the SM. There are five Higgs bosons - two charged H^\pm and three neutral ones: the CP-even h and H and CP-odd A . Couplings of the physical Higgs bosons to fermions and gauge bosons have standard forms as for the 2HDM, with the Model I Yukawa interaction.

Masses of scalars are as follows (see, e.g. [17, 2])

$$M_{H^\pm}^2 = -\frac{\lambda_4 + \lambda_5}{2} v^2, \quad M_A^2 = -v^2 \lambda_5, \quad (v^2 = v_S^2 + v_D^2). \quad (35)$$

The neutral CP-even mass matrix is equal to

$$\mathcal{M} = \begin{pmatrix} \lambda_1 v_S^2 & \lambda_{345} v_S v_D \\ \lambda_{345} v_S v_D & \lambda_2 v_D^2 \end{pmatrix}. \quad (36)$$

⁶Sometimes called a *normal extremum* N , see e.g. [16]

The mass matrix (36) gives masses of the neutral CP-even Higgs bosons:

$$M_{h,H}^2 = \frac{\lambda_1 v_S^2 + \lambda_2 v_D^2 \pm \sqrt{(\lambda_1 v_S^2 + \lambda_2 v_D^2)^2 - 4 \det \mathcal{M}}}{2}, \quad (37)$$

with sign + for the H and sign – for h .

References

- [1] N. G. Deshpande and E. Ma, Phys. Rev. D **18** (1978) 2574; R. Barbieri, L. J. Hall and V. S. Rychkov, Phys. Rev. D **74** (2006) 015007 [arXiv:hep-ph/0603188].
- [2] I. F. Ginzburg and K. A. Kanishev, Phys. Rev. D **76** (2007) 095013 [arXiv:0704.3664 [hep-ph]].
- [3] I. F. Ginzburg, I. P. Ivanov and K. A. Kanishev, Phys. Rev. D **81** (2010) 085031 [arXiv:0911.2383 [hep-ph]].
- [4] I. P. Ivanov, Acta Phys. Polon. B **40** (2009) 2789 [arXiv:0812.4984 [hep-ph]].
- [5] I. F. Ginzburg, K.A. Kanishev, M. Krawczyk, D. Sokolowska, Phys. Rev. D **82**, 123533 (2010) [arXiv:1009.4593 [hep-ph]]
- [6] D. Sokołowska: Dark Matter data and constraints on the quartic coupling (work in progress)
- [7] G. Belanger, F. Boudjema, A. Pukhov and A. Semenov, Comput. Phys. Commun. **176** (2007) 367 [arXiv:hep-ph/0607059]. G. Belanger, F. Boudjema, A. Pukhov and A. Semenov, arXiv:0803.2360 [hep-ph]. G. Belanger, F. Boudjema, A. Pukhov and A. Semenov, Comput. Phys. Commun. **174** (2006) 577 [arXiv:hep-ph/0405253]. G. Belanger, F. Boudjema, A. Pukhov and A. Semenov, Comput. Phys. Commun. **149** (2002) 103 [arXiv:hep-ph/0112278].
- [8] Q. H. Cao, E. Ma and G. Rajasekaran, Phys. Rev. D **76** (2007) 095011 [arXiv:0708.2939 [hep-ph]]; P. Agrawal, E. M. Dolle and C. A. Krenke, Phys. Rev. D **79**, 015015 (2009) [arXiv:0811.1798 [hep-ph]]; M. Gustafsson, E. Lundstrom, L. Bergstrom and J. Edsjo, Phys. Rev. Lett. **99** (2007) 041301 [arXiv:astro-ph/0703512];
- [9] E. M. Dolle and S. Su, Phys. Rev. D **80** (2009) 055012 [arXiv:0906.1609 [hep-ph]]; E. Dolle, X. Miao, S. Su and B. Thomas, Phys. Rev. D **81**, 035003 (2010) [arXiv:0909.3094 [hep-ph]];
- [10] L. Lopez Honorez, E. Nezri, J. F. Oliver and M. H. G. Tytgat, JCAP **0702** (2007) 028 [arXiv:hep-ph/0612275]; C. Arina, F. S. Ling and M. H. G. Tytgat, JCAP **0910** (2009) 018 [arXiv:0907.0430 [hep-ph]]; T. Hambye and M. H. G. Tytgat, Phys. Lett. B **659** (2008) 651 [arXiv:0707.0633 [hep-ph]]; E. Nezri, M. H. G. Tytgat and G. Vertongen, JCAP **0904** (2009) 014 [arXiv:0901.2556 [hep-ph]]; S. Andreas, M. H. G. Tytgat and Q. Swillens, JCAP **0904** (2009) 004 [arXiv:0901.1750 [hep-ph]]; S. Andreas, T. Hambye and M. H. G. Tytgat, JCAP **0810** (2008) 034 [arXiv:0808.0255 [hep-ph]]; L. L. Honorez and C. E. Yaguna, arXiv:1003.3125 [hep-ph];
- [11] E. Lundstrom, M. Gustafsson and J. Edsjo, Phys. Rev. D **79** (2009) 035013 [arXiv:0810.3924 [hep-ph]].
- [12] M. Krawczyk and D. Sokołowska, arXiv:0911.2457 [hep-ph].
- [13] Particle Data Group. *Journ. of Phys.* **G 37** #7A (2010) 075021
- [14] I. Ginzburg (private communication); I.Ginzburg, K.Kanishev, M.Krawczyk, D.Sokołowska (work in progress)

- [15] M. B. Gavela, O. Pene, N. Rius and S. Vargas-Castrillon, Phys. Rev. D **59** (1999) 025008 [arXiv:hep-ph/9801244];
- [16] J. L. Diaz-Cruz and A. Mendez, Nucl. Phys. B **380** (1992) 39. P. M. Ferreira, R. Santos and A. Barroso, Phys. Lett. B **603**, 219 (2004) [Erratum-ibid. B **629**, 114 (2005)] [arXiv:hep-ph/0406231]; A. Barroso, P. M. Ferreira and R. Santos, Phys. Lett. B **632**, 684 (2006) [arXiv:hep-ph/0507224]. A. Barroso, P. M. Ferreira and R. Santos, Phys. Lett. B **652**, 181 (2007) [arXiv:hep-ph/0702098]; A. Barroso, P. M. Ferreira, R. Santos and J. P. Silva, Phys. Rev. D **74** (2006) 085016 [arXiv:hep-ph/0608282].
- [17] I. F. Ginzburg and M. Krawczyk, Phys. Rev. D **72** (2005) 115013 [arXiv:hep-ph/0408011].
- [18] D. Sokołowska, arXiv:1009.5099v1 [hep-ph]
- [19] L. L. Honorez, C. E. Yaguma, arXiv:1011.1411 [hep-ph]